

Decomposition of Tertiary Alkoxy Radicals

By Michael Buback*, Matthias Kling**, and Stefan Schmatz

Institut für Physikalische Chemie, Georg-August-Universität Göttingen,
Tammannstraße 6, D-37077 Göttingen, Germany

Dedicated to the memory of Prof. Dr. Dr. h.c. Ernst Ulrich Franck

(Received March 31, 2005; accepted May 10, 2005)

Tertiary Alkoxy Radicals / Peroxide Decomposition / Density Functional Theory

Rate coefficients of β -scission reactions in tertiary alkoxy radicals, $R(\text{CH}_3)_2\text{CO}$ ($R = \text{methyl, ethyl, } \textit{tert}\text{-butyl and } \textit{neo}\text{-pentyl}$) have been estimated *via* density functional theory (DFT) calculations in conjunction with statistical unimolecular rate theory. For *tert*-butoxy, results obtained by employing different basis sets are compared with experimental values, indicating that UB3LYP/6-31G(d,p) excellently predicts kinetic data. Rate coefficients for inter- and intramolecular hydrogen abstraction are also reported. Depending on R , the β -scission rate may vary by orders of magnitude. The predicted temperature dependence of the alcohol-to-ketone product ratios for alkoxy radical decomposition in a hydrocarbon environment is in remarkably close agreement with the corresponding ratios measured on the product mixtures from decomposition of *tert*-butyl and *tert*-amyl peroxyacetates in solution of *n*-heptane.

1. Introduction

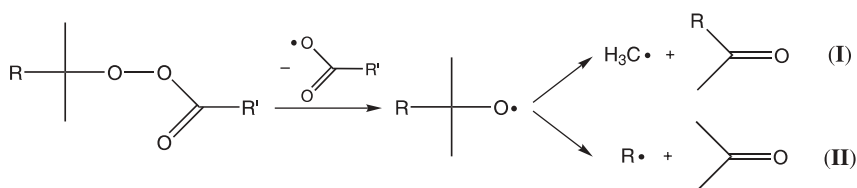
Organic peroxyesters of general structure $R(\text{CH}_3)_2\text{CO-OC(O)R}'$, with R and R' being alkyl moieties, are widely used as initiators in free-radical polymerizations [1–4]. Dissociation of the peroxy bond yields an alkoxy radical $R-(\text{CH}_3)_2\text{CO}\cdot$ and a carbonyloxy radical $\cdot\text{OC(O)-R}'$. Both species may undergo β -scission reactions, by which oxygen-centered radicals are converted into carbon-centered ones. These secondary decomposition reactions may result in a decrease of initiator efficiency and may affect the microstructure of the final polymer, as oxygen- and carbon-centered radicals differ in chain-transfer activity [4]. Whereas recombination of the primary $R-(\text{CH}_3)_2\text{CO}\cdot$

* Corresponding author. E-mail: mbuback@gwdg.de

** *Present address:* FOM Institute for Atomic and Molecular Physics (AMOLF),
Kruislaan 407, 1098 SJ Amsterdam, The Netherlands

and $\cdot\text{OC}(\text{O})\text{-R}'$ radicals does not affect initiator efficiency, as the peroxyester molecule is recovered, radical-radical reactions in which species produced by β -scission of $\text{R-(CH}_3)_2\text{CO}\cdot$ and/or $\cdot\text{OC}(\text{O})\text{-R}'$ are engaged may result in a loss of radicals and thus in a lowering of initiator efficiency, as the products of such reactions are thermally stable under typical polymerization conditions. A reduction of initiator efficiency will occur in cases where such β -scission C–C bond breaking reactions occur as in-cage processes on a sub-ns time-scale, *i.e.* during a period in which the two radical species from peroxide decomposition are in close proximity. Although the kinetics of thermally and photochemically induced peroxide decomposition reactions have been extensively addressed in the past [1, 2, 4–6], the implications of the decay dynamics of radical intermediates on initiator efficiency have not been investigated in any detail so far.

Detailed investigations into the mechanism and the time-scales of decarboxylation of carbonyloxy radicals $\cdot\text{OC}(\text{O})\text{-R}'$, to yield CO_2 and the radical $\text{R}'\cdot$, have been reported [5–9]. Recently, the combination of several ultrafast spectroscopic techniques with theoretical modeling on the basis of DFT calculations has provided detailed insight into the decarboxylation mechanism of aryl carbonyloxy radicals [6]. In both experimental [4–6, 9] and theoretical [6, 10] studies, the mechanism and the rate of decarboxylation of $\cdot\text{OC}(\text{O})\text{-R}'$, with R' being phenyl, naphthyl, phenyloxy or benzyl, were found to crucially depend on the stability of the substituent $\text{R}'\cdot$.



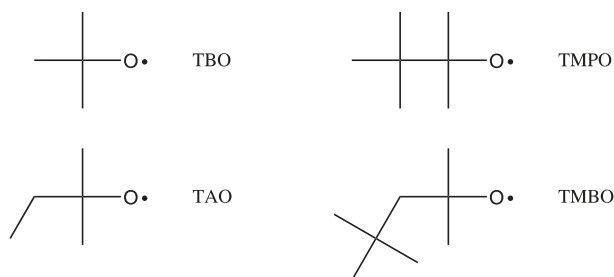
Scheme 1. Simplified scheme of sequential dissociation reactions occurring with peroxyesters. R and R' are alkyl moieties. The present article focuses on β -scission-type C–C bond breaking processes of the alkoxy radical intermediate $\text{R(CH}_3)_2\text{CO}\cdot$ for which two reaction pathways, **I** and **II**, are indicated.

The present contribution focuses on DFT-based estimates of thermal rate coefficients for β -scission reactions of tertiary alkoxy radicals. Such species occur in chemically initiated radical polymerizations. As displayed in Scheme 1, $\text{R-(CH}_3)_2\text{CO}\cdot$ radicals from decomposition of peroxyesters (or from dialkyl peroxides) may undergo β -scission reactions along two pathways, producing either a methyl radical + the ketone $\text{R-C}(\text{O})\text{CH}_3$ (channel **I**), or an alkyl radical $\text{R}\cdot$ + acetone (channel **II**). Additional reaction channels for alkoxy radicals are isomerization [11–14] and, in condensed phase, are reactions with

$\cdot\text{OC}(\text{O})\text{-R}'$ or with $\text{R}'\cdot$, which latter radical is produced by decarboxylation of $\cdot\text{OC}(\text{O})\text{-R}'$. Moreover, the alkoxy radical may abstract hydrogen from solvent molecules (channel **III**) [15, 16]. To ensure close correspondence of the obtained data, a unimolecular reaction is considered for channel **III**, where abstraction takes place in a solvent-complexed alkoxy radical species. Propane is used as the complexing agent, because this molecule is the smallest hydrocarbon with secondary hydrogen atoms. As was shown by Atkinson [13] and Blitz *et al.* [17], isomerization may be neglected for small alkoxy radicals, but may be very fast in cases where a 1,5-hydrogen shift *via* a six-membered transition structure may take place (channel **IV**) [11, 14]. The rate coefficients for intermolecular H-abstraction were found to be almost insensitive to the structure of the alkoxy radical [16].

Because of the eminent relevance of alkoxy radicals in atmospheric chemistry [13], several theoretical studies into the decomposition of these species have already been carried out. Rate coefficients have been reported for the decomposition of the *tert*-butoxy radical [18–20], of linear alkoxy radicals with up to five carbon atoms [21], and of a series of linear and branched alkoxy radicals [18, 19]. Density functional theory (DFT) calculations [18–20] and compound methods such as CBS-RAD [18] and G2 theory in its variants G2(MP2) [20] and G2(MP2,SVP) [21] have been used for modeling experimental kinetic data [17, 20, 22, 23] *via* statistical rate theories. Within the study into alkoxy radicals containing up to five carbon atoms [19], quantum-chemical calculations have been performed employing the *ab initio* BAC-MP4 method and DFT using the B3LYP hybrid functional with the polarized double-zeta 6-31G(d,p) basis set. The decomposition of the *tert*-butoxy radical that has been extensively studied in the past [13, 17, 19, 20, 22, 23], but also of *tert*-amyloxy (2-methyl-2-butoxy) [19], may serve for evaluating the reliability of the applied electronic structure methods for predicting β -scission rates. For this reason, within the present study, the decomposition rate of these two alkoxy radicals has been estimated *via* DFT calculations. The present study focuses on *tert*-alkyloxy radicals which are of relevance for chemically induced free-radical polymerization. In addition to reactions of *tert*-butoxy and *tert*-amyloxy radicals, the decomposition kinetics of alkoxy radicals with $\text{R}\cdot = \text{tert-butyl}$ (1,1,2,2-tetramethyl propyloxy) and $\text{R}\cdot = \cdot\text{CH}_2\text{-tert-butyl}$ (1,1,3,3-tetramethyl butyloxy) is of importance. Data for these two larger radicals are reported here for the first time.

The paper is organized as follows: Sect. 2 describes the methodology. The results from quantum-chemical calculations and the Arrhenius parameters for thermal decomposition reactions of *tert*-butoxy (TBO), *tert*-amyloxy (TAO), 1,1,2,2-tetramethyl propyloxy (TMPO), and 1,1,3,3-tetramethyl butyloxy (TMBO) radicals (see Scheme 2) are presented and discussed in Sect. 3, where the data for TBO and TAO is also correlated with product distributions measured for the decomposition of *tert*-butyl peroxyacetate and *tert*-amyl peroxyacetate in liquid *n*-heptane [24].



Scheme 2. Structures of the alkoxy radicals under investigation: *tert*-butoxy (TBO), *tert*-amyloxy (TAO), 1,1,2,2-tetramethyl propyloxy (TMPO), and 1,1,3,3-tetramethyl butyloxy (TMBO).

2. Methodology

The determination of reaction barriers and reaction energies for the β -scission-type C–C bond breaking of tertiary alkoxy radicals is based on density functional theory (DFT) calculations. The adequate description of the transition state for β -scission of alkoxy radicals requires the inclusion of a large part of the electron correlation energy. Since in the present case an open-shell species dissociates into a closed-shell species plus an open-shell fragment, non-dynamical electron correlation is not expected to play a major role. A considerable fraction of dynamical electron correlation is included in UMP2 or UB3LYP [25, 26] calculations. In particular for larger systems, the latter method usually provides good agreement with experimental data at low cost [27]. As a reference, we used the recently developed G3//B3LYP [27] procedure for the calculation of the energetics of the TBO radical employing the UB3LYP/6-31G(d) geometry and zero-point energy (ZPE) including single-point energy calculations up to the MP2(full)//GTLarge level.

The program package Gaussian03 [28] was used for the quantum-chemical calculations reported here. The structures of the relevant stationary points (reactants, products, and first-order saddle points for reaction) on the potential energy surfaces (PESs) of the alkoxy radicals were fully optimized employing the UB3LYP functional in conjunction with basis sets up to 6-311+G(d,p). To confirm that true minima on the PESs have been found, the Hessian matrices at the stationary points were calculated. The TS routine of Gaussian03 and the intrinsic reaction coordinate (IRC) method [29, 30] have been used to confirm the transition state (first-order saddle point) geometries.

As the present study aims at the understanding of β -scission reactions in larger radicals, it appears preferable to use the relatively small 6-31G(d,p) basis set. An assessment of the quality of the predictions obtained by employing this basis set is obtained by comparison with available experimental data for the *tert*-butoxy radical (TBO). The polarization functions on the hydrogen atom, which are almost without any influence on the decomposition of TBO,

are crucial for the adequate description of the hydrogen abstraction processes (channels **III** and **IV**). The 6-31G(d,p) basis was also used in the work by Méreau *et al.* [11, 19].

Calculated harmonic vibrational frequencies and equilibrium rotational constants are used to derive the thermal contributions to enthalpies and entropies of reaction and activation, respectively. A point of debate is the inclusion of reaction path degeneracies into the statistical reaction rate expressions. They may originate from the symmetry factor in the rotational partition function of the reactant. While from a naive point of view, C_{3v} symmetry is anticipated for the *tert*-butoxy radical, the symmetry is lost in the doubly degenerate 2E electronic ground state due to Jahn–Teller coupling which, in addition, lifts the degeneracy of the 2E electronic ground state [31]. As a consequence, neither for rotational symmetry nor for ground state degeneracy, factors have been included into the expressions for the partition functions used in our calculations. Moreover, the actual dynamics should include both sheets of the PES, not only for the reactant species, but also for all situations along the way to dissociation. Thus it would be incorrect to include electronic degeneracy only for the reactant. An investigation of the dynamic Jahn–Teller effect of the *tert*-butoxy radical has not been reported so far, while there are several studies into the simpler, structurally related methoxy radical ($\text{CH}_3\text{O}\cdot$) [32–35]. However, even in this much smaller system, a thorough investigation of the vibronically fully coupled dynamics at higher internal energies, close to dissociation into formaldehyde and a hydrogen atom, is still beyond reach.

It is well known that unrestricted single-determinant wave functions (such as unrestricted Hartree–Fock, UHF) may exhibit a considerable spin contamination in radicals [36, 37]. Although such a contamination from higher-spin excited states would certainly affect the molecular geometries and the energetics, it was shown that spin contamination in unrestricted density functional calculations is usually small (no spin contamination would occur in DFT calculations if the exact functionals were known) [38–40]. Hybrid density functionals such as B3LYP have a somewhat higher spin contamination due to the admixture of Hartree–Fock exchange. In all our calculations, the deviation of the average $\langle S^2 \rangle$ values from the eigenvalues $S(S+1) = 0.75$ does not exceed 5%. Thus spin contamination does not affect our results to a significant extent.

3. Results and discussion

3.1 Energetics of β -scission and H-transfer reactions of alkoxy radicals

Barrier heights and reaction energies for reaction of the radicals TBO, TAO, TMPO and TMBO along the relevant channels of each species have been calculated *via* UB3LYP using various types of basis sets. The results are summarized in Table 1. The influence of the selected basis set on barrier heights

Table 1. Relative energies of reactants, transition states and products (in kJ mol^{-1}) for the C–C bond β -scission of TBO, TAO, TMPO, and TMBO radicals. The energy of the reactants is set to zero for all methods and basis sets used in the calculations. E_{el} and E_{elr} denote electronic energies, while E_0 includes corrections due to zero-point vibrational effects (harmonic level) and $\Delta_r H^\circ(298\text{ K})$ is the reaction enthalpy. Absolute energy values in hartrees are available from the authors upon request. Channels **I** and **II** are illustrated in Scheme 1. Channel **III** refers to abstraction of a secondary H atom from propane, the smallest hydrocarbon molecule with secondary H atoms, which has been chosen for the DFT calculations. Channel **IV** refers to intramolecular isomerization *via* a 1,5-H shift reaction to produce a carbon-centered hydroxyl radical.

System	channel	reaction	basis set ^a	barrier height		reaction energy/enthalpy	
				E_{el}	E_0	E_{elr}	$\Delta_r H^\circ(298\text{ K})$
TBO	I=II	$(\text{CH}_3)_3\text{CO} \rightarrow \text{CH}_3 + \text{CH}_3\text{C}(\text{O})\text{CH}_3$	6-31G(d)	69.6	58.5	32.0	15.6
			6-31+G(d)	64.7	54.2	22.2	6.4
			SVP	67.6	56.8	25.1	8.9
			6-31G(d,p)	68.7	57.7	30.7	14.5
			6-31+G(d,p)	63.6	53.2	20.0	4.5
			6-311+G(d,p)	60.0	49.9	14.2	-1.4
			G3B3 ^b	64.8	54.0	28.3	12.7
	III	$(\text{CH}_3)_3\text{CO} \cdot \text{C}_3\text{H}_8 \rightarrow (\text{CH}_3)_3\text{COH} + \text{C}_3\text{H}_7$	6-31G(d,p)	35.3	22.2	-3.4	-12.3
TAO	I	$\text{C}_2\text{H}_5(\text{CH}_3)_2\text{CO} \rightarrow \text{CH}_3 + \text{C}_2\text{H}_5\text{C}(\text{O})\text{CH}_3$	6-31G(d,p)	66.2	55.7	25.7	9.7
	II	$\text{C}_2\text{H}_5(\text{CH}_3)_2\text{CO} \rightarrow \text{C}_2\text{H}_5 + \text{CH}_3\text{C}(\text{O})\text{CH}_3$	6-31G(d,p)	50.7	41.4	13.5	-1.1
	III	$\text{C}_2\text{H}_5(\text{CH}_3)_2\text{CO} \cdot \text{C}_3\text{H}_8 \rightarrow \text{C}_2\text{H}_5(\text{CH}_3)_2\text{COH} + \text{C}_3\text{H}_7$	6-31G(d,p)	35.9	22.2	-3.1	-12.2
TMPO	I	$\text{C}_4\text{H}_9(\text{CH}_3)_2\text{CO} \rightarrow \text{CH}_3 + \text{C}_4\text{H}_9\text{C}(\text{O})\text{CH}_3$	6-31G(d,p)	65.5	55.5	20.0	4.5
	II	$\text{C}_4\text{H}_9(\text{CH}_3)_2\text{CO} \rightarrow \text{C}_4\text{H}_9 + \text{CH}_3\text{C}(\text{O})\text{CH}_3$	6-31G(d,p)	23.8	17.0	-32.8	-45.0
	III	$\text{C}_4\text{H}_9(\text{CH}_3)_2\text{CO} \cdot \text{C}_3\text{H}_8 \rightarrow \text{C}_4\text{H}_9(\text{CH}_3)_2\text{COH} + \text{C}_3\text{H}_7$	6-31G(d,p)	41.6	27.9	2.2	-7.2
TMBO	I	$\text{C}_5\text{H}_{11}(\text{CH}_3)_2\text{CO} \rightarrow \text{CH}_3 + \text{C}_5\text{H}_{11}\text{C}(\text{O})\text{CH}_3$	6-31G(d,p)	60.6	51.1	14.0	-1.6
	II	$\text{C}_5\text{H}_{11}(\text{CH}_3)_2\text{CO} \rightarrow \text{C}_5\text{H}_{11} + \text{CH}_3\text{C}(\text{O})\text{CH}_3$	6-31G(d,p)	39.1	32.1	-2.9	-16.4
	III	$\text{C}_5\text{H}_{11}(\text{CH}_3)_2\text{CO} \cdot \text{C}_3\text{H}_8 \rightarrow \text{C}_5\text{H}_{11}(\text{CH}_3)_2\text{COH} + \text{C}_3\text{H}_7$	6-31G(d,p)	38.7	26.8	2.2	-5.8
IV	$\text{C}_5\text{H}_{11}(\text{CH}_3)_2\text{CO} \rightarrow \text{C}_5\text{H}_{10}(\text{CH}_3)_2\text{COH}$	6-31G(d,p)	46.1	33.0	7.0	5.1	

^a Unless otherwise stated, the functional UB3LYP was used throughout these calculations. ^b Compound method for energy calculation based on the UB3LYP/6-31G(d) geometry and ZPE [27].

and reaction enthalpies will first be investigated for the β -scission reaction of the *tert*-butoxy radical. (Results obtained for the other radicals upon varying the basis set may be obtained from the authors upon request).

Using the 6-31G(d), 6-31G(d,p), and SVP basis sets yields very similar barrier heights, E_{el} , for TBO. They differ by at most 2 kJ mol^{-1} , with the number obtained employing the 6-31G(d,p) basis set being in between the two other values. Inclusion of diffuse functions (6-31+G(d) instead of 6-31G(d) and 6-31+G(d,p) instead of 6-31G(d,p) basis sets), decreases the barrier height by about 5 kJ mol^{-1} . Applying the triple-zeta basis 6-311+G(d,p) further lowers the barrier by about another 4 kJ mol^{-1} . The barrier height deduced from G3B3 almost coincides with the one obtained using the 6-31+G(d) basis. Comparison of the E_{el} and $E_{\text{el,r}}$ values for TBO in Table 1 indicates that the effects of basis set selection on the electronic reaction energies, $E_{\text{el,r}}$, are about twice as large as the ones on barrier heights, E_{el} , e.g., a difference of about 18 kJ mol^{-1} results for $E_{\text{el,r}}$, in passing from the 6-31G(d) to the 6-311+G(d,p) basis set. This effect is partly due to the basis set superposition error (BSSE).

The barrier heights corrected for zero-point vibrational energy, E_0 , are by about 10 kJ mol^{-1} below the associated electronic energies, E_{el} , for the β -scission reaction. This effect is essentially due to the loss of one vibrational degree of freedom in the transition state. The $\Delta_r H^\circ$ (298 K) values are by about 16 kJ mol^{-1} below the associated electronic energies at 0 K, $E_{\text{el,r}}$, as two product species are formed with their additional rotational and translational degrees of freedom providing larger thermochemical contributions than vibrational modes.

The experimental reaction enthalpy for β -scission of *tert*-butoxy is available from measured standard enthalpies of formation: $-90.4 \text{ kJ mol}^{-1}$ for *tert*-butoxy [41], $-218.5 \text{ kJ mol}^{-1}$ for acetone [42], and $145.7 \text{ kJ mol}^{-1}$ for methyl [43]. The resulting value of $\Delta_r H^\circ$ (298 K) = 17.6 kJ mol^{-1} is remarkably close to the numbers estimated by DFT using the 6-31G(d) and 6-31G(d,p) basis sets, which are 15.6 and 14.5 kJ mol^{-1} , respectively. Interestingly, the $\Delta_r H^\circ$ (298 K) value deduced employing the larger triple-zeta basis set 6-311+G(d,p) differs by as much as 19 kJ mol^{-1} from the experimental value and would even suggest an exothermic reaction.

The multitude of basis sets has also been used for estimating the barrier heights and reaction energies of channel **III** for TBO and of all relevant reaction channels for the radicals TAO, TMPO and TMBO. The resulting data shows the same trends as outlined for TBO. Because of the remarkable quality of predictions *via* UB3LYP in conjunction with the 6-31G(d,p), only results deduced *via* this basis set will be discussed in what follows and are presented in Table 1.

The barrier height for the intermolecular H-transfer reaction between TBO and propane, to yield *tert*-butanol, is significantly below the one for the β -scission reaction. Zero-point energy effects decrease the barrier for the bimolecular channel **III** to a slightly larger extent, by about 13 kJ mol^{-1} ,

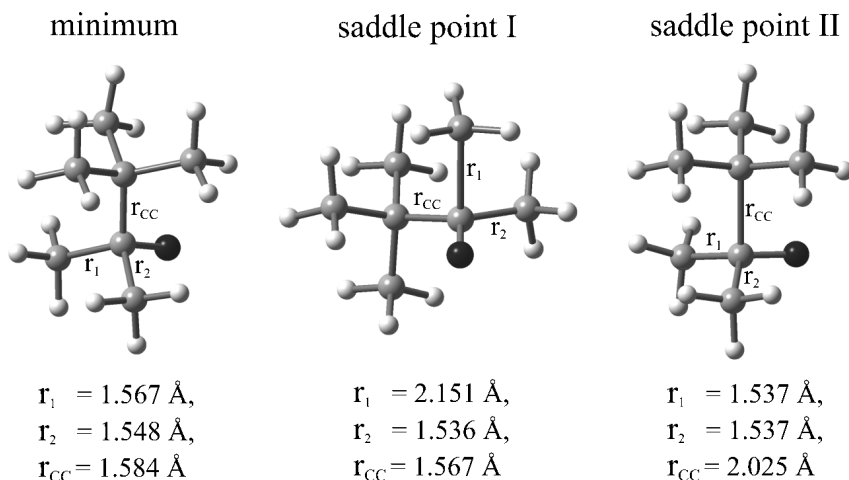


Fig. 1. Optimized geometries of the tetramethyl propyloxy (TMPO) radical and of the saddle points toward methyl + 3,3-dimethylbutyl ketone (**I**) and *tert*-butyl + acetone (**II**) formation (results from UB3LYP/6-31G(d,p)).

than the one for unimolecular β -scission (channel **I**). Due to formation of a strong O–H bond, the H-abstraction reaction is exothermic, $\Delta_r H^\circ$ (298 K) = $-12.3 \text{ kJ mol}^{-1}$.

The barrier for channel **I** with TAO is slightly below the associated TBO value (Table 1). The barrier of the channel **II** β -scission in TAO is by about 14 kJ mol^{-1} below the channel **I** value. Hydrogen abstraction of TAO from propane shows almost the same energetics as the channel **III** reaction for TBO.

Fig. 1 illustrates the optimized geometries of the tetramethyl propyloxy (TMPO) radical and of the associated saddle points toward formation of methyl + 3,3-dimethylbutyl ketone (channel **I**) and of *tert*-butyl + acetone (channel **II**), as obtained by UB3LYP calculations using the 6-31G(d,p) basis set. In the saddle point structure for channel **I**, the breaking C–C bond is elongated by about 0.58 \AA , whereas this distance is slightly shorter in the channel **II** saddle point structure. Fig. 2 presents the corresponding information for decomposition of the tetramethyl butyloxy (TMBO) radical *via* saddle point **I**, to yield methyl + 4,4-dimethyl-2-pentanone, and *via* saddle point **II**, to yield *neo*-pentyl + acetone.

The barrier heights E_0 for methyl loss (channel **I**) are close to each other for TMPO and TAO. A considerably lower barrier is, however, obtained for the channel **II** reaction with TMPO, in which the relatively stable *tert*-butyl radical is produced. The latter process is the most exothermic one of all the reactions considered in this work.

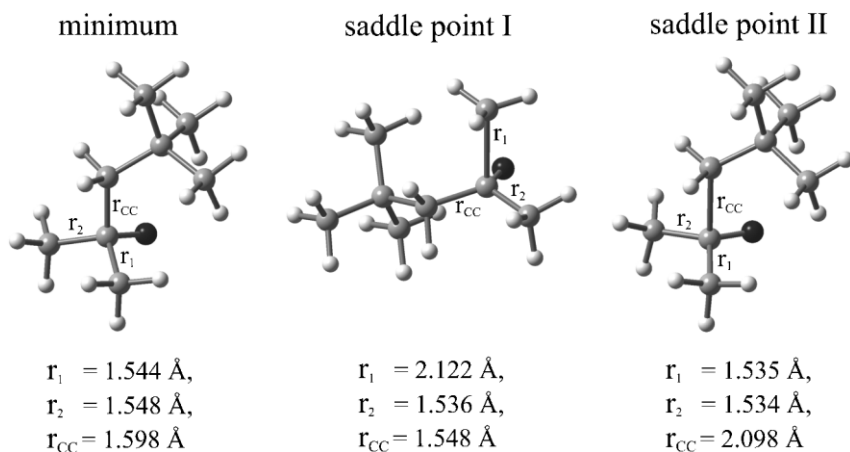


Fig. 2. Optimized geometries of the tetramethyl butyloxy (TMBO) radical and of the saddle points toward methyl + 4,4-dimethyl-2-pentanone (**I**) and *neo*-pentyl + acetone (**II**) formation (results from UB3LYP/6-31G(d,p)).

For TMBO, β -scission according to channel **I** exhibits an E_0 barrier which is slightly, by about 5 kJ mol^{-1} , below the associated TAO value. The barrier toward acetone formation (channel **II**), $E_0(\text{TMBO})$, is by about 9 kJ mol^{-1} below the TAO value, but is by 15 kJ mol^{-1} above $E_0(\text{TMPO})$. The barrier toward hydrogen abstraction (channel **III**) for TMBO is slightly above the corresponding TAO value.

In Ref. [16], it was stated that the rate coefficients for intermolecular H-abstraction were almost insensitive toward the structure of the alkoxy radical. Inspection of the entries for the channel **III** reactions in Table 1 indicates that this statement is supported by our DFT results, although the energy barrier for this reaction slightly increases in going from TBO, TAO to TMBO and to TMPO. The barrier estimated for the intramolecular 1,5-H shift reaction of TMBO (channel **IV**) is slightly above the one for intermolecular hydrogen abstraction (channel **III**) of the same radical.

3.2 Kinetics of β -scission and H-transfer reactions of alkoxy radicals

Among the four alkoxy radicals under investigation, TBO has been most widely studied so far. Before addressing the β -scission and H-transfer reactions of the entire group of alkoxy radicals, the TBO rate parameters obtained by using different basis sets for the UB3LYP calculations will be compared with the available experimental material. Arrhenius parameters, A and E_a , and rate coefficients, k , for 298 K are presented in Table 2. Temperature-dependent rate coefficients $k(T)$ between 200 and 700 K have been estimated on the basis of

our quantum-chemical data employing transition state theory:

$$k(T) = \frac{k_{\text{B}}T}{h} \frac{Q_{\text{vib}}^{\ddagger} Q_{\text{rot}}^{\ddagger}}{Q_{\text{vib}} Q_{\text{rot}}} \exp\left(-\frac{E_0}{RT}\right), \quad (1)$$

where k_{B} and R denote Boltzmann's constant and the gas constant, respectively. Q and Q^{\ddagger} are the vibrational and rotational partition functions of reactants and transition states, respectively. The parameters A and E_a are obtained from fits of $k(T)$ to the Arrhenius expressions $k(T) = A \exp(-E_a/RT)$. The resulting Arrhenius parameters and $k(298 \text{ K})$ values are listed in Table 2. The pre-exponentials, A , are almost insensitive toward the basis set used for the estimates of geometries and vibrational frequencies. The resulting numbers are in close agreement with the pre-exponential $A = 1 \times 10^{14} \text{ s}^{-1}$ obtained or adopted by other groups [18, 20]. As is to be expected from the calculated barrier heights in Table 1, the activation energies obtained *via* the 6-31G(d), 6-31G(d,p), and SVP basis sets are close to each other and are clearly above the numbers obtained by using the diffuse functions or the triple-zeta basis set. Inspection of the Arrhenius rate coefficients for ambient temperature, $k(298 \text{ K})$ tells that the numbers deduced *via* the 6-31G(d), 6-31G(d,p), and SVP basis sets are in good agreement with the experimental data [17, 20, 22, 23]. The $k(298 \text{ K})$ value estimated *via* the extended triple-zeta basis is by more than one order of magnitude above the experimental values. Méreau *et al.* recently proposed the structure–activity relationship (SAR) with a fixed value of $A = L^{\ddagger} \times 10^{14} \text{ s}^{-1}$ to be used in conjunction with barrier heights estimated from UB3LYP/6-31G(d,p) [19]. Applying this strategy to *tert*-butoxy, with a reaction path degeneracy of $L^{\ddagger} = 3$, results in a clear overestimate of the β -scission rate coefficients, as may be seen from Table 2 and also from Fig. 3, where an Arrhenius plot of TBO β -scission rate coefficient is shown. The rate coefficients deduced from UB3LYP in conjunction with 6-31G(d), 6-31G(d,p), and with SVP yield good estimates of the experimental data. The line in Fig. 3 which represents β -scission rate obtained *via* the 6-31G(d,p) basis appears as if this were the line fitted to the entire set of experimental data. This noticeable agreement of calculated and measured data provides a further strong argument for using UB3LYP/6-31G(d,p) toward estimating the kinetics of alkoxy radical reactions. While this finding is in agreement with results of Méreau *et al.* [19], obtained from a structure–activity-relationship for tertiary alkoxy radicals, we propose to use calculated pre-exponentials without an additional degeneracy factor (owing to the Jahn–Teller effect, see methodology Sect. 2), resulting in values close to $A = 1 \times 10^{14} \text{ s}^{-1}$ and in a much better agreement with the experimental rate data.

The rate parameters follow the trends suggested by the calculated barrier heights presented in Table 1. The pre-exponential factors of the β -scission reactions according to either channel **I** or **II** are around $1 \times 10^{14} \text{ s}^{-1}$. $k(298 \text{ K})$ for

Table 2. *Upper seven rows:* Arrhenius parameters, A and E_a , and rate coefficients for 298 K deduced from a fit of temperature-dependent rate coefficients between 200 and 700 K for β -scission of *tert*-butoxy to methyl + acetone (channel **I** \equiv **II**) estimated *via* transition state theory on the basis of rate parameters from UB3LYP/6-31G(d,p) and G3B3 theory; *Rows 8 to 12:* Reported experimental values (8 to 11) and data estimated *via* the structure–activity relationship (SAR) (from Ref. [19]).

Method	$A/10^{14} \text{ s}^{-1}$	$E_a/(\text{kJ mol}^{-1})$	$k(298 \text{ K})/10^3 \text{ s}^{-1}$
UB3LYP/6-31G(d)	1.3	63.4	1.0
UB3LYP/6-31+G(d)	1.2	59.0	5.7
UB3LYP/SVP	1.2	61.6	2.0
UB3LYP/6-31G(d,p)	1.3	62.6	1.4
UB3LYP/6-31+G(d,p)	1.2	57.9	8.4
UB3LYP/6-311+G(d,p)	1.1	54.6	30
G3B3	1.3	58.9	6.1
Fittschen <i>et al.</i> (2000) [20]	1.0	60.5	2.5
Blitz <i>et al.</i> (1999) [17]	0.14	57.0	1.4
Batt <i>et al.</i> (1989) [22]	1.1	62.5	1.2
Choo and Benson (1981) [23]	1.3	64.0	0.8
SAR	3.0	59.4	12

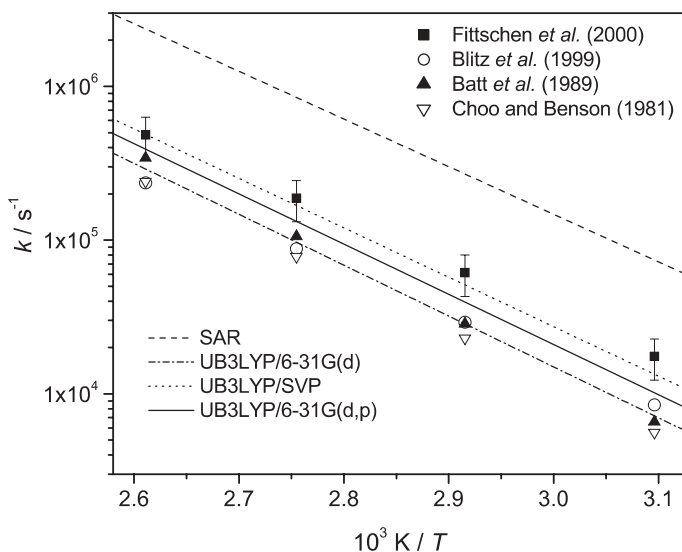


Fig. 3. Arrhenius plots for β -scission of the *tert*-butoxy radical. Individual points represent experimental data taken from literature [20] and data points according to experimentally obtained Arrhenius parameters [17, 22, 23]. The dashed line indicates data derived from the structure–activity-relationship (SAR) proposed by Méreau *et al.* [19]. The other straight lines result from our DFT estimates using different types of basis sets.

Table 3. Arrhenius parameters, A and E_a , and rate coefficients at 298 K for reactions of the alkoxy radicals TBO, TAO, TMBO, and TMPO. The data is deduced from Arrhenius fitting of temperature-dependent rate coefficients between 200 and 700 K, which have been estimated *via* transition state theory on the basis of rate parameters from UB3LYP/6-31G(d,p).

System	channel	reaction	A/s^{-1}	$E_a/$ (kJ mol $^{-1}$)	$k(298\text{ K})/$ s^{-1}
TBO	I≡II	$(\text{CH}_3)_3\text{CO} \rightarrow \text{CH}_3 + \text{CH}_3\text{C}(\text{O})\text{CH}_3$	1.3×10^{14}	62.6	1.4×10^3
	III	$(\text{CH}_3)_3\text{CO} \cdots \text{C}_3\text{H}_8 \rightarrow (\text{CH}_3)_3\text{COH} + \text{C}_3\text{H}_7$	3.6×10^{10}	22.7	3.7×10^6
TAO	I	$\text{C}_2\text{H}_5(\text{CH}_3)_2\text{CO} \rightarrow \text{CH}_3 + \text{C}_2\text{H}_5\text{C}(\text{O})\text{CH}_3$	1.3×10^{14}	60.4	3.3×10^3
	II	$\text{C}_2\text{H}_5(\text{CH}_3)_2\text{CO} \rightarrow \text{C}_2\text{H}_5 + \text{CH}_3\text{C}(\text{O})\text{CH}_3$	1.1×10^{14}	45.7	1.0×10^6
	III	$\text{C}_2\text{H}_5(\text{CH}_3)_2\text{CO} \cdots \text{C}_3\text{H}_8 \rightarrow \text{C}_2\text{H}_5(\text{CH}_3)_2\text{COH} + \text{C}_3\text{H}_7$	8.0×10^{10}	23.1	7.3×10^6
TMPO	I	$\text{C}_4\text{H}_9(\text{CH}_3)_2\text{CO} \rightarrow \text{CH}_3 + \text{C}_4\text{H}_9\text{C}(\text{O})\text{CH}_3$	7.9×10^{13}	60.0	2.4×10^3
	II	$\text{C}_4\text{H}_9(\text{CH}_3)_2\text{CO} \rightarrow \text{C}_4\text{H}_9 + \text{CH}_3\text{C}(\text{O})\text{CH}_3$	1.1×10^{14}	20.8	2.5×10^{10}
	III	$\text{C}_4\text{H}_9(\text{CH}_3)_2\text{CO} \cdots \text{C}_3\text{H}_8 \rightarrow \text{C}_4\text{H}_9(\text{CH}_3)_2\text{COH} + \text{C}_3\text{H}_7$	4.7×10^{10}	28.9	4.0×10^5
TMBO	I	$\text{C}_5\text{H}_{11}(\text{CH}_3)_2\text{CO} \rightarrow \text{CH}_3 + \text{C}_5\text{H}_{11}\text{C}(\text{O})\text{CH}_3$	5.6×10^{13}	55.3	1.1×10^4
	II	$\text{C}_5\text{H}_{11}(\text{CH}_3)_2\text{CO} \rightarrow \text{C}_5\text{H}_{11} + \text{CH}_3\text{C}(\text{O})\text{CH}_3$	4.6×10^{13}	35.6	2.7×10^7
	III	$\text{C}_5\text{H}_{11}(\text{CH}_3)_2\text{CO} \cdots \text{C}_3\text{H}_8 \rightarrow \text{C}_5\text{H}_{11}(\text{CH}_3)_2\text{COH} + \text{C}_3\text{H}_7$	1.0×10^{10}	26.8	2.0×10^5
	IV	$\text{C}_5\text{H}_{11}(\text{CH}_3)_2\text{CO} \rightarrow \text{C}_5\text{H}_{10}(\text{CH}_3)_2\text{COH}$	2.9×10^{12}	33.5	3.8×10^6

the channel **II** reaction increases by orders of magnitude in going from TBO, *via* TAO and TMBO to TMPO. This enormous change reflects the increasing stability of the alkyl radical produced by the β -scission reaction. That the differences in decomposition rate coefficients of alkoxy radicals are primarily due to activation energies rather than to pre-exponentials is consistent with earlier findings [13, 18, 19].

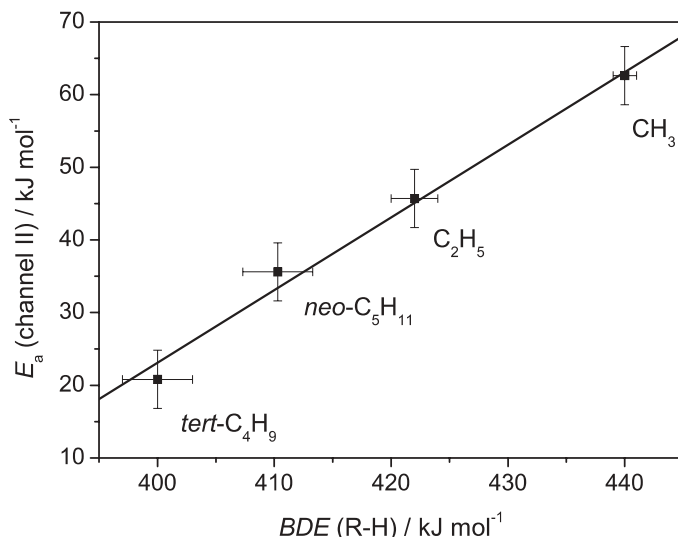


Fig. 4. Evans–Polanyi correlation of the activation energy for the β -scission reaction, *via* channel II, of alkoxy radicals with the bond dissociation energy, $BDE(R-H)$ of the associated hydrocarbons $R-H$. The activation energies are obtained from UB3LYP/6-31G(d,p) calculations. The $BDEs$ are taken from literature [44] or are estimated according to Benson’s rules. The solid line represents a linear fit with slope unity.

In Fig. 4, the so-called Evans–Polanyi plot is presented, in which the activation energy for decomposition of the alkoxy radicals *via* channel II is plotted against the bond dissociation energy, $BDE(R-H)$, which is a measure of the stability of the alkyl radical $R\cdot$ produced by “de-acetonization” of the alkoxy radicals. The close fit of the data *via* the straight line with slope unity is strongly indicative of (i) the Evans–Polanyi correlation being suitable for analysis and prediction of β -scission rates of the radicals under investigation and of (ii) the DFT calculations on the UB3LYP/6-31G(d,p) level providing excellent estimates of the activation energies of these radical decomposition reactions.

The intermolecular hydrogen-abstraction rates (channel III reactions in Table 3) are less sensitive toward the specific type of radical, which finding has already been reported [16]. However, for the two larger radicals, TMPO and TMBO, which have been studied here for the first time, a clearly lower abstraction rate than for the small-size alkoxy radicals is predicted by our DFT calculations. The studies into TMBO also allow for estimates of the rate of 1,5-H-shift (channel IV) relative to the intermolecular H-abstraction reaction within the alkoxy radical–propane complex (channel III). Although the activation energy for channel IV is higher, the intramolecular 1,5-H shift reaction occurs at a higher rate. This effect which is due to the much larger

pre-exponential factor (Table 3) becomes even more pronounced at higher temperatures. The Arrhenius parameters for the 1,5-H shift with TMBO are in excellent agreement with previous studies on alkoxy radicals, where a hydrogen atom was abstracted from a CH₃ group [11, 13, 21]. Note that the Arrhenius parameters were found to be significantly different, when H-abstraction occurs from CH₂ or CH-groups. The rate coefficients increase within the series CH₃ < CH₂ < CH [11, 13]. A tunneling correction factor of 2.7 was suggested to be used for the intramolecular H-abstraction from CH₃-groups in alkoxy radicals at 298 K [11]. Taking this correction into account, we obtain a rate constant close to $k(298\text{ K}) = 1.0 \times 10^7\text{ s}^{-1}$ for channel **IV** with TMBO.

The data presented in Table 3 constitutes a large body of information on gas-phase kinetics of *tert*-butoxy radicals. It is tempting to use this data also for modelling kinetics in the dense fluid or liquid state of non-polar materials, *e.g.*, of radical reactions in hydrocarbon solution or during free-radical polymerizations, such as fluid-phase ethene polymerization.

Although solvent effects, in particular in polar environments, are known to result in smaller activation energies for channels **I** to **III** with alkoxy radicals [15, 16], the β -scission rate coefficients in Table 3 might be helpful for estimating the extent of in-cage radical–radical termination after the primary peroxyester decomposition step in condensed non-polar fluid phase. Such termination reactions reduce initiator efficiency and thus may affect the economics of the polymerization process. The situation may be visualized by taking free-radical ethene polymerizations initiated by three peroxyacetates into account, *e.g.*, by *tert*-butyl peroxyacetate (TBPA), *tert*-amyl peroxyacetate (TAPA), and tetramethylpropyl peroxyacetate (TMPPA). The acetyloxy radical, which is one of the two primary species from peroxyacetate decomposition, is relatively stable with the half-life for decarboxylation most likely exceeding the time period of about one nanosecond during which the two primary radicals remain in a caged situation. Whether irreversible radical recombination and/or disproportionation reactions, *i.e.* processes other than the back-reaction to the parent peroxyacetate, will take place during this short in-cage period, primarily depends on the β -scission rate of the associated alkoxy radical. This β -scission reaction produces a carbon-centered radical which may readily react with the acetyloxy radical. Estimating (from the parameters listed in Table 3) half-lives for the β -scission channel **II** at a typical ethene polymerization temperature of 200 °C yields: 36 ns for TBO, 0.6 ns for TAO, and 40 ps for TMPO. These numbers suggest that, in case of initiation by TBPA, the undesired in-cage reaction between the acetyloxy radical and a methyl radical from TBO decomposition will not occur to a large extent and initiator efficiency thus should be high. For TMPPA, on the other hand, alkoxy decomposition will occur as a very fast in-cage process. As a consequence, a large fraction of radicals will be lost by in-cage reaction between acetyloxy and *tert*-butyl radicals and initiator efficiency will be significantly below the one of TBPA-initiated polymerization. The efficiency in

case of initiation by TAPA should be intermediate between the situations occurring with TBPA and TMPPA. These trends, suggested by the data in Table 3, are indeed consistent with what is experimentally observed in ethene high-pressure polymerizations [45–47]. It is beyond the scope of this article to quantitatively analyze initiator efficiency on the basis of the rate coefficients from DFT. Work in this area which additionally requires consideration of in-cage dynamics of bimolecular reactions is currently underway in our laboratory [48, 49].

The applicability of the DFT-derived rate coefficients toward the prediction of reaction rates in non-polar environment may also be checked by inspection of product distributions from peroxyester decomposition in hydrocarbon solution. Such experiments have been carried out for a series of peroxyesters dissolved in *n*-heptane within a wide range of pressures and temperatures [24, 50]. The alcohol-to-ketone product ratio has been determined gas-chromatographically after complete peroxyester decomposition. For comparison with the rate data in Table 3, the product distributions obtained for decomposition of *tert*-butyl peroxyacetate and of *tert*-amyl peroxyacetate are of particular interest. As the acetyloxy radical will not undergo reactions that yield either the alcohol or the ketone species produced during TBO or TAO decomposition in hydrocarbon solution, the measured alcohol-to-ketone product ratio should be essentially determined by the ratio of channel **III** to channel **II** rates. As the strategy for treating bimolecular H-abstraction reactions (channel **III**) has not yet been adequately worked out, the comparison will not be made *via* absolute concentration ratios, but by the temperature dependence of the measured alcohol-to-ketone product concentrations. Arrhenius plots of the gas-chromatographically measured alcohol-to-ketone product ratios yield straight lines with the slope being given by the difference in activation energies, $\Delta E_a(\text{ol/on})$, of intramolecular H-abstraction (“ol”-formation according to channel **III**) and β -scission (“on”-formation according to channel **II**). The experimental values deduced from decomposition studies carried out at 500 bar are:

$$\Delta E_a(\text{ol/on}) = -36.4 \text{ kJ mol}^{-1} \text{ for TBO (from TBPA decomposition) and}$$

$$\Delta E_a(\text{ol/on}) = -18.1 \text{ kJ mol}^{-1} \text{ for TAO (from TAPA decomposition) [24].}$$

These values are to be compared with the energy differences deduced from the UB3LYP/6-31G(d,p) calculations. As the picture underlying the calculations of channel **III** kinetics (in which a solvent-complexed radical reacts and releases the solvent molecule thereby gaining translational and rotational degrees of freedom) is not appropriate for reactions in dense liquid phase, the comparison is made *via* the energy barriers E_0 (listed in Table 1). The so-obtained energy differences between channels **III** and **II** are:

$$\Delta E_0(\text{ol/on}) = -35.5 \text{ kJ mol}^{-1} \text{ for TBO and}$$

$$\Delta E_0(\text{ol/on}) = -19.2 \text{ kJ mol}^{-1} \text{ for TAO.}$$

The almost perfect agreement of experimentally determined and DFT-derived differences in energy barriers for both TBO and TAO provides another strong argument for applying UB3LYP/6-31G(d,p) toward estimates of rate coefficients for reactions of alkoxy radicals. It should further be noted, that the DFT-derived number for TBO, $\Delta E_0(\text{ol/on}) = -35.5 \text{ kJ mol}^{-1}$, is in excellent agreement with the experimental value of $\Delta E_a(\text{ol/on}) = -36.6 \text{ kJ mol}^{-1}$ that follows from the associated literature rate data for β -scission and H-abstraction from cyclohexane dissolved in benzene [15].

For a full understanding of initiator efficiency in free-radical polymerizations, the complex sequence of radical reactions subsequent to peroxide decomposition should be analyzed on the basis of rate data from DFT calculations on the UB3LYP/6-31G(d,p) level and special attention should be paid to aspects of bimolecular in-cage reactivity.

4. Conclusions

Rate coefficients of β -scission in tertiary alkoxy radicals, $\text{R}(\text{CH}_3)_2\text{CO}\cdot$, with R being methyl, ethyl, *tert*-butyl, and *neo*-pentyl, have been estimated *via* density functional theory (DFT) calculations. The structures of the relevant stationary points on the potential energy surfaces of reactants, products, and first-order saddle points were fully optimized. For the *tert*-butoxy radical, results from DFT calculations using several basis sets were checked against experimental values. The comparison shows that UB3LYP/6-31G(d,p) allows for excellent predictions of kinetic data. The quantum-chemical data serve as input parameters for the determination of temperature-dependent rate coefficients, $k(T)$, which were obtained within the framework of transition state theory. The $\text{R}(\text{CH}_3)_2\text{CO}\cdot$ radicals occur as primary intermediates in the decomposition of peroxyesters and dialkyl peroxides which are important initiators of free-radical polymerization. Depending on the type of R-group, the scission rate of the C–C bond in β -position to the radical functionality may vary by orders of magnitude. Rapid β -scission of $\text{R}(\text{CH}_3)_2\text{CO}\cdot$ favors in-cage radical–radical combination and disproportionation reactions, which reduce initiator efficiency in chemically induced polymerizations. For $\text{R}(\text{CH}_3)_2\text{CO}\cdot$ also rate coefficients for intermolecular hydrogen abstraction, from propane, were estimated *via* UB3LYP/6-31G(d,p). This data, in conjunction with the calculated β -scission rate coefficients, allows for an estimate of alcohol-to-ketone product ratios associated with reactions of alkoxy radicals in a hydrocarbon environment. The predicted temperature dependence of this ratio is found to be in remarkably close agreement with alcohol-to-ketone ratios measured on the product mixtures from decomposition of *tert*-butyl and *tert*-amyl peroxyacetates in solution of *n*-heptane. For the tetramethyl butyloxy radical, also the kinetics of the intramolecular 1,5-hydrogen shift reaction has been estimated *via* DFT.

Acknowledgement

The authors are grateful to the Deutsche Forschungsgemeinschaft (SFB 357 “*Molekulare Mechanismen Unimolekularer Prozesse*”) and to AKZO Nobel (Polymer Chemicals Research Center Deventer) for generous support. Discussions with Professor Karlheinz Hoyer mann are gratefully acknowledged.

References

1. K. Fujimori, in *Organic Peroxides*, W. Ando (Ed.), Wiley, New York (1992) p. 319.
2. Y. Sawaki, in *Organic Peroxides*, W. Ando (Ed.), Wiley, New York (1992) p. 425.
3. C. A. Barson and J. C. Bevington, *J. Polym. Sci. A: Polym. Chem.* **35** (1997) 2955.
4. M. Buback and J. Sandmann, *Z. Phys. Chem.* **214** (2000) 583.
5. J. Wang, T. Tateno, H. Sakuragi, and K. Tokumaru, *J. Photochem. Photobiol.* **92** (1995) 53.
6. M. Buback, M. Kling, S. Schmatz, and S. Schroeder, *Phys. Chem. Chem. Phys.* **6** (2004) 5441.
7. J. Chateaufneuf, J. Luszyk, and K. U. Ingold, *J. Am. Chem. Soc.* **110** (1988) 2886.
8. M. Buback, M. Kling, M. T. Seidel, F.-D. Schott, J. Schroeder, and U. Steegmüller, *Z. Phys. Chem.* **215** (2001) 717.
9. J. Aßmann, M. Kling, and B. Abel, *Angew. Chem. Int. Ed.* **42** (2003) 2226.
10. M. Kling and S. Schmatz, *Phys. Chem. Chem. Phys.* **5** (2003) 3891.
11. R. Méreau, M.-T. Rayez, F. Caralp, and J.-C. Rayez, *Phys. Chem. Chem. Phys.* **5** (2003) 4828.
12. H. Somnitz and R. Zellner, *Phys. Chem. Chem. Phys.* **2** (2000) 1899.
13. R. Atkinson, *Int. J. Chem. Kinet.* **29** (1997) 99.
14. D. Johnson, P. Cassanelli, and R. A. Cox, *J. Phys. Chem. A* **108** (2004) 519.
15. M. Weber and H. Fischer, *J. Am. Chem. Soc.* **121** (1999) 7381.
16. D. V. Avila, C. E. Brown, K. U. Ingold, and J. Luszyk, *J. Am. Chem. Soc.* **115** (1993) 466.
17. M. Blitz, M. J. Pilling, S. H. Robertson, and P. W. Seakins, *Phys. Chem. Chem. Phys.* **1** (1999) 73.
18. A. Rauk, R. J. Boyd, S. L. Boyd, D. J. Henry, and L. Radom, *Can. J. Chem.* **81** (2003) 431.
19. R. Méreau, M.-T. Rayez, F. Caralp, and J.-C. Rayez, *Phys. Chem. Chem. Phys.* **2** (2000) 3765.
20. C. Fittschen, H. Hippler, and B. Viskolcz, *Phys. Chem. Chem. Phys.* **2** (2000) 1677.
21. H. Somnitz and R. Zellner, *Phys. Chem. Chem. Phys.* **2** (2000) 1907.
22. L. Batt, M. W. M. Hisham, and M. Mackay, *Int. J. Chem. Kinet.* **21** (1989) 535.
23. K. Y. Choo and S. W. Benson, *Int. J. Chem. Kinet.* **13** (1981) 833.
24. D. Nelke, *Diploma Thesis*, Universität Göttingen (1999).
25. A. D. Becke, *J. Chem. Phys.* **98** (1993) 5648.
26. C. Lee, W. Yang, and R. G. Parr, *Phys. Rev. B* **37** (1988) 785.
27. A. G. Baboul, L. A. Curtiss, P. C. Redfern, and K. Raghavachari, *J. Chem. Phys.* **110** (1999) 7650.
28. M. J. Frisch, G. W. Trucks, H. B. Schlegel, G. E. Scuseria, M. A. Robb, J. R. Cheeseman, J. A. Montgomery, Jr., T. Vreven, K. N. Kudin, J. C. Burant, J. M. Millam, S. S. Iyengar, J. Tomasi, V. Barone, B. Mennucci, M. Cossi, G. Scalmani, N. Rega, G. A. Petersson, H. Nakatsuji, M. Hada, M. Ehara, K. Toyota, R. Fukuda, J. Hasegawa, M. Ishida, T. Nakajima, Y. Honda, O. Kitao, H. Nakai, M. Klene, X. Li, J. E. Knox, H. P. Hratchian, J. B. Cross, V. Bakken, C. Adamo, J. Jaramillo,

- R. Gomperts, R. E. Stratmann, O. Yazyev, A. J. Austin, R. Cammi, C. Pomelli, J. W. Ochterski, P. Y. Ayala, K. Morokuma, G. A. Voth, P. Salvador, J. J. Dannenberg, V. G. Zakrzewski, S. Dapprich, A. D. Daniels, M. C. Strain, O. Farkas, D. K. Malick, A. D. Rabuck, K. Raghavachari, J. B. Foresman, J. V. Ortiz, Q. Cui, A. G. Baboul, S. Clifford, J. Cioslowski, B. B. Stefanov, G. Liu, A. Liashenko, P. Piskorz, I. Komaromi, R. L. Martin, D. J. Fox, T. Keith, M. A. Al-Laham, C. Y. Peng, A. Nanayakkara, M. Challacombe, P. M. W. Gill, B. Johnson, W. Chen, M. W. Wong, and C. Gonzalez, J. A. Pople, Gaussian 03, Revision B.04, Gaussian, Inc.: Wallingford CT (2004).
29. C. Gonzales and H. B. Schlegel, *J. Chem. Phys.* **90** (1989) 2154.
 30. C. Gonzales and H. B. Schlegel, *J. Phys. Chem.* **94** (1990) 5523.
 31. B. K. Janousek, A. H. Zimmerman, K. J. Reed, and J. I. Brauman, *J. Am. Chem. Soc.* **100** (1978) 6142.
 32. J. Schmidt-Klügmann, H. Köppel, S. Schmatz, and P. Botschwina, *Chem. Phys. Lett.* **369** (2003) 21.
 33. T. A. Barckholtz and T. A. Miller, *Int. Rev. Phys. Chem.* **17** (1998) 435.
 34. U. Hoeper, P. Botschwina, and H. Köppel, *J. Chem. Phys.* **112** (2000) 4132.
 35. A. V. Marenich and J. E. Boggs, *Chem. Phys. Lett.* **404** (2005) 351.
 36. J. Cioslowsky, G. Liu, M. Martinov, P. Piskorz, and D. Moncrief, *J. Am. Chem. Soc.* **118** (1996) 5261.
 37. J. Pacansky, B. Liu, and D. DeFrees, *J. Org. Chem.* **51** (1986) 3720.
 38. J. Baker, A. Scheiner, and J. Andzelm, *Chem. Phys. Lett.* **216** (1993) 380.
 39. G. J. Laming, N. C. Handy, and R. D. Amos, *Mol. Phys.* (1993) 1121.
 40. J. M. Wittbrodt and H. B. Schlegel, *J. Chem. Phys.* **105** (1996) 6574.
 41. D. F. McMillen and D. M. Golden, *Ann. Rev. Phys. Chem.* **33** (1982) 493.
 42. K. B. Wiberg, L. S. Crocker, and K. M. Morgan, *J. Am. Chem. Soc.* **113** (1991) 3447.
 43. M. W. J. Chase, *J. Phys. Chem. Ref. Data* **9** (1998) 1.
 44. J. A. M. Simoes, J. F. Liebmann, A. Greenberg (Eds.), *Energetics of Organic Free Radicals*, Blackie Academic & Professional, London (1996).
 45. S. Hinrichs, *Diploma Thesis*, Universität Göttingen (2000).
 46. P. Becker, M. Buback, and J. Sandmann, *Macromol. Chem. Phys.* **203** (2002) 2113.
 47. M. Buback, *Macromol. Symp.* **182** (2002) 103.
 48. S. Hinrichs, *Dissertation*, Universität Göttingen (2005).
 49. M. Buback, S. Hinrichs, S. Jauer, M. Kling, and S. Schmatz, in preparation.
 50. M. Buback, D. Nelke, and H. P. Vögele, in preparation.